ARTICLES

Journal of Semiconductors
(2023) 44, 082202
doi: 10.1088/1674-4926/44/8/082202

Highly efficient organic solar cells with improved stability enabled by ternary copolymers with antioxidant side chains

Ao Song‡, Qiri Huang‡, Chunyang Zhang, Haoran Tang, Kai Zhang, Chunchen Liu†, Fei Huang†, and Yong Cao

Institute of Polymer Optoelectronic Materials and Devices, State Key Laboratory of Luminescent Materials and Devices, South China University of Technology (SCUT), Guangzhou 510640, China

Abstract: The stability of organic solar cells (OSCs) remains a major concern for their ultimate industrialization due to the photo, oxygen, and water susceptibility of organic photoactive materials. Usually, antioxidant additives are blended as radical scavengers into the active layer. However, it will induce the intrinsic morphology instability and adversely affect the efficiency and long-term stability. Herein, the antioxidant dibutylhydroxytoluene (BHT) group has been covalently linked onto the side chain of benzothiadiazole (BT) unit, and a series of ternary copolymers D18-Cl-BTBHTx (x = 0, 0.05, 0.1, 0.2) with varied ratio of BHT-containing side chains have been synthesized. It was found that the introduction of BHT side chains would have a negligible effect on the photophysical properties and electronic levels, and the D18-Cl-BTBHT0.05: Y6-based OSC achieved the highest power conversion efficiency (PCE) of 17.6%, which is higher than those based active layer blended with BHT additives. More importantly, the unencapsulated device based on D18-Cl-BTBHTx (x = 0.05, 0.1, 0.2) retained approximately 50% of the initial PCE over 30 hours operation under ambient conditions, significantly outperforming the control device based on D18-Cl (90% degradation in PCE after 30 h). This work provides a new structural design strategy of copolymers for OSCs with simultaneously improved efficiency and stability.

Key words: organic solar cells; ternary copolymers; antioxidant side chain; photostability

Citation: A Song, Q R Huang, C Y Zhang, H R Tang, K Zhang, C C Liu, F Huang, and Y Cao, Highly efficient organic solar cells with improved stability enabled by ternary copolymers with antioxidant side chains[J]. *J. Semicond.*, 2023, 44(8), 082202. https://doi.org/10.1088/1674-4926/44/8/082202

1. Introduction

Organic solar cells (OSCs) show promising application prospects in building integrated photovoltaics and wearable electronic equipment due to their merits of light weight, flexibility, and solution processability[1–19]. Tremendous efforts, including high-performance active layer materials development[20–22] and device structures innovation[23], have been devoted to promoting the power conversion efficiency (PCE) of single-junction OSC devices to an unprecedented level over 19%[24, 25]. However, despite the substantial achievement on improving the PCE of OSCs, stability is still one of the most important issues need to be considered for the ultimate industrialization of OSCs[26–31]. Generally, the instability or degradation of OSCs can be divided into several catalogues according to the practical operating conditions, including mechanical instability under stretching and bending, light stability under irradiation, air instability under oxygen (O_2) and moisture (H_2O) invasion, burn-in instability and thermal instability under heating, and so on[28]. In particular, the deterioration of OSCs under continuous irradiation and H_2O and O_2 has been recognized as a major challenge to prolonging the operating lifetime to meet the commercialization standard.

Researchers have recently endeavored to explore strategies for improving the stability of OSCs under continuous irradiation and H_2O and O_2 invasion[32, 33]. The encapsulation of OSCs has proven to be effective to prevent the invasion of H_2O and O_2, and eventually improve the lifetime of prepared devices[34–36]. Together with the degradation caused by H_2O and O_2 diffusion, the photooxidation of active layer is usually another key pathway to deteriorate the performance of OSCs. The major photodegradation pathways of organic semiconductors have been reported to include triplet mediated singlet oxygen generation or anion mediated superoxide radical anion formation, which make them undergo an irreversible radical oxidative degradation process[37, 38]. Over the past few decades, various approaches have been proposed to improve the photostability of OSCs, among which the most prevalent one is the introduction of antioxidant media as the radical scavengers into the active layer[39–41]. Usually, antioxidants have been widely adopted as the additive into active layer to terminate the radicals for suppressing the degradation of the photosensitive materials, resulting in the increase of OSCs stability. For example, hindered phenol-based antioxidants have frequently been used as the stabilizing additives to improve the photostability of OSCs. It was demonstrated that hydrogen could transfer from phenol hydroxyl group to the alkylperoxyls originated from the oxidation of polymers, which would break the chain reaction of photooxidation and eventually terminate the degradation of conjugated polymers[41]. However,

Ao Song and Qiri Huang contributed equally to this work and should be considered as co-first authors.

Correspondence to: C C Liu, mscliu@scut.edu.cn; F Huang, msfhuang@scut.edu.cn

Received 15 FEBRUARY 2023; Revised 15 MARCH 2023.

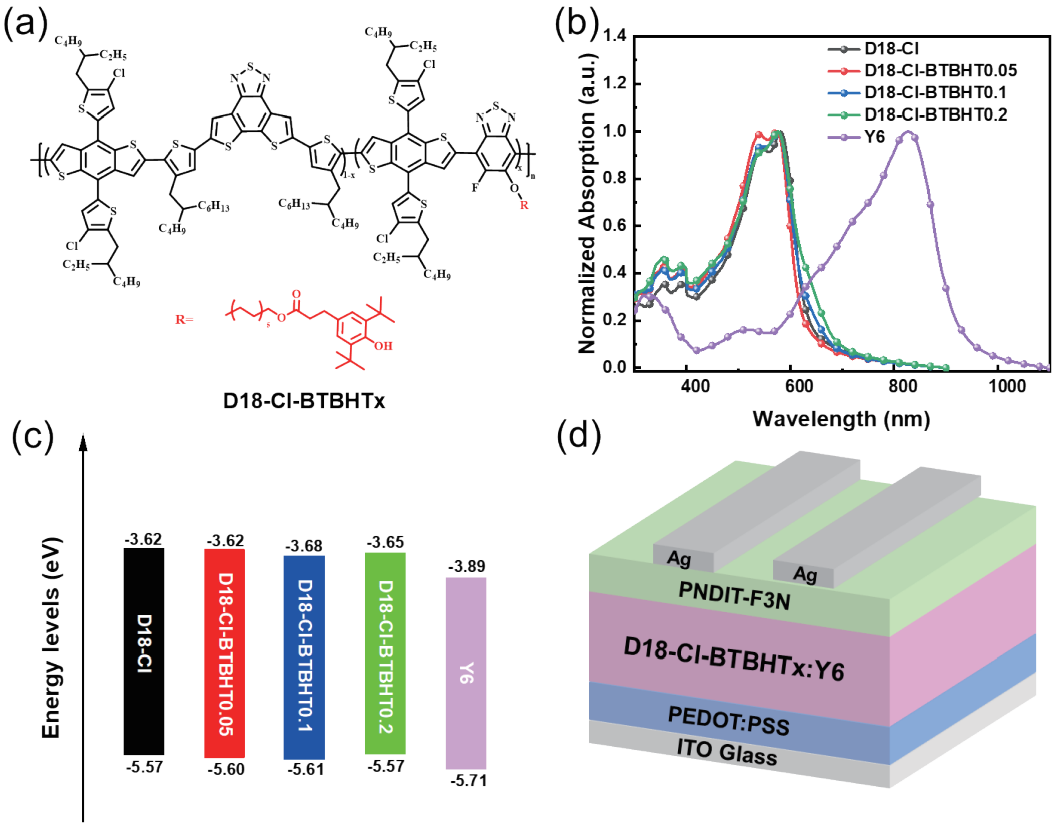

Fig. 1. (Color online) (a) Chemical structures of the copolymers D18-Cl-BTBHTx (x = 0, 0.05, 0.1, 0.2); (b) absorption spectra of D18-Cl, D18-Cl-BTBHT0.05, D18-Cl-BTBHT0.1, D18-Cl-BTBHT0.2 and Y6 in films; (c) schematic illustration of energy levels of D18-Cl, D18-Cl-BTBHT0.05, D18-Cl-BTBHT0.1, D18-Cl-BTBHT0.2 and Y6; (d) device architecture of OSCs employed in this study.

adding antioxidants *via* physical blending was found to adversely affect the long-term morphology stability because of the spontaneous aggregation of antioxidants, thus decreasing the efficiency and long-term stability of OSCs[37, 41]. Therefore, it is of great significance to design conjugated polymers linking with antioxidants *via* covalent bonds to prevent the free movement of antioxidants, and eventually achieve the goal of increasing the photostability and long-term stability of OSCs without sacrificing efficiency.

Herein, the dibutylhydroxytoluene (BHT) group with antioxidizing capability is linked *via* an ester reaction onto the side chain of benzothiadiazole (BT) unit. The molar ratio of this BT unit with a BHT side chain is incorporated into the conjugated backbone of the widely-used polymer donor D18-Cl[42, 43]. As a result, a series of ternary copolymers D18-Cl-BTBHTx (x = 0, 0.05, 0.1, 0.2) have been successfully designed and synthesized, and ternary copolymerization have been demonstrated as an efficient method in tuning compatibility, solubility, and stability of copolymers[44–46]. It has been found that the introduction of BHT group would have a negligible effect on optical, thermal, and electrochemical properties of the obtained copolymers. The OSCs prepared with D18-Cl-BTBHTx (x = 0, 0.05, 0.1, 0.2): Y6 exhibited the comparable PCEs, and the highest PCE of 17.6% could be achieved for the D18-Cl-BTBHT0.05: Y6-based device. More importantly, the D18-Cl-BTBHTx (x = 0.05, 0.1, 0.2)-based devices showed much enhanced photooxidation stability. The unencapsulated device retained approximately 50% of the initial PCE over 30 hours operation under ambient conditions, which was significantly higher than that of the control group based on D18-Cl (90% degradation in PCE after 30 h). Furthermore, the carrier-generation, charge recombination and transport of OSCs before and after irradiation were investigated, revealing that the introduction of BHT side chains could successfully reduce the trap-assisted recombination after long-term operation, and thus improve the photostability of OSCs. This work provides a feasible strategy to develop ternary copolymers for OSCs with simultaneously improved efficiency and stability.

2. Results and discussion

2.1. Design, synthesis, and characterization of D18-Cl-BTBHTx

As shown in Fig. 1(a), the design of copolymers D18-Cl-BTBHTx is derived from the D18-Cl, which is a previously reported high-efficiency donor polymer[42, 43]. Innovatively, different molar ratios of the BT unit with antioxidant BHT group terminated side chain were copolymerized to afford a series of donor polymers with antioxidation capability: D18-Cl-BTBHT0.05, D18-Cl-BTBHT0.1 and D18-Cl-BTBHT0.2, respectively. The detailed synthesis procedures are illustrated in Scheme S1 (Supporting Information) and all of the intermediates were characterized with $^{1}H/^{13}C$ NMR spectroscopy, the correlated data are shown in Figs. S1–S14. The introduction of BHT-terminated side chain will induce negligible influence on the solubility and molecular weight of obtained ternary copolymers. All of the synthesized polymers D18-Cl-BTBHTx can be readily dissolved in common organic solvents, such as chloroform (CF) and chlorobenzene (CB), at room temperature. The

Table 1. Molecular weights, optical properties, and electronic energy levels of copolymers D18-Cl-BTBHTx (x = 0, 0.05, 0.1, 0.2).

Polymer	Mn (kDa)	PDI	λ_{max}[a] (nm)	λ_{onset}[a] (nm)	E_g^{opt}[b] (eV)	E_{ox} (V)	E_{HOMO}[c] (eV)	E_{LUMO}[d] (eV)
D18-Cl	58.0	2.3	545, 580	636	1.95	1.16	−5.57	−3.62
D18-Cl-BTBHT0.05	58.2	1.9	540, 574	626	1.98	1.19	−5.60	−3.62
D18-Cl-BTBHT0.1	49.8	1.6	541, 576	642	1.93	1.20	−5.61	−3.68
D18-Cl-BTBHT0.2	49.9	1.9	540, 576	646	1.92	1.16	−5.57	−3.65

[a] In films. [b] $E_g^{opt} = 1240/\lambda_{onset}$. [c] $E_{HOMO} = -(E_{ox} - E_{(Fc/Fc^+)} + 4.8)$ eV, [d] $E_{LUMO} = E_{HOMO} + E_g^{opt}$.

molecular weights (M_n) of D18-Cl-BTBHTx were determined in the range of 40 to 50 kDa with a polydispersion index (PDI) of ~2.0 by gel permeation chromatography (GPC) at 150 °C with the eluent of 1,2,4-trichlorobenzene (Fig. S15 in the Supporting Information). The thermal properties of D18-Cl-BTBHTx were evaluated by thermogravimetric analysis (TGA) and differential scanning calorimetry (DSC) measurements (Fig. S16, Supporting Information). The 5% weight loss temperatures of D18-Cl, D18-Cl-BTBHT0.05, D18-Cl-BTBHT0.1, D18-Cl-BTBHT0.2 were measured to be 436, 435, 418, and 405 °C, respectively, which indicate the good thermal stability of D18-Cl-BTBHTx. The DSC traces of these polymers showed no obvious melting or crystallization peaks in the temperature range of 25–300 °C. This suggests that the incorporation of BHT-terminated side chain would not affect the thermodynamic transition of obtained D18-Cl-BTBHTx.

The effect of introducing BT unit with BHT-terminated side chain on the photophysical properties of obtained ternary copolymers was first investigated. As shown in Fig. 1(b), ternary copolymers D18-Cl-BTBHTx (x = 0.05, 0.1, 0.2) showed similar absorption spectra with the D18-Cl, which are well complementary with absorption of the non-fullerene acceptor Y6. A similar absorption peak at ~580 nm with a shoulder peak at ~540 nm could be observed for these four copolymers and a similar absorption onset at ~635 nm could be obtained, which endows these copolymers with the almost identical optical band gap (E_g^{opt}) of ~1.95 eV. Noteworthy, after scrutinizing the absorption intensity in the range of 600–750 nm of these copolymers, it could be observed that the absorption in this range was gradually enhanced by increasing the copolymerizing ratio of the BT unit. This increased absorption in the long-wavelength region is speculated to be ascribed to the enhanced intramolecular charge transfer along the conjugated backbone caused by the stronger electron-deficient character of the BT unit.

The electrochemical properties of all polymers were further evaluated by cyclic voltammetry (CV) (Fig. S17, Supporting Information) and the estimated energy diagram is plotted in Fig. 1(c). Both the highest occupied molecular orbital (HOMO) and lowest unoccupied molecular orbital (LUMO) levels of copolymers D18-Cl-BTBHTx (x = 0.05, 0.1, 0.2) were similar to those of D18-Cl, which indicates that the introduction of reasonable ratio of BT unit with antioxidant side chain will not significantly change the electronic energy levels of the obtained copolymers. The relevant molecular weights, and optical and electrochemical data are summarized in Table 1.

In addition, the effect of incorporating BT unit with antioxidant BHT terminated side chain on the photostability of blend active layer was further investigated and the absorption spectra of blend films of D18-Cl-BTBHTx: Y6 were monitored in real time under continuous illumination. As shown in Fig. 2, the absorption decreases in the range of 530–600 nm caused by the degradation of copolymer D18-Cl-BTBHTx was gradually suppressed by increasing the copolymerizing ratio of antioxidant BT unit from 0 to 20%. This result strongly demonstrates the efficacy of introducing BHT terminated side chains to improve the photooxidation stabilization ability of blend films within OSCs.

2.2. Performance of OSCs

The effect of introducing BHT side chains on the performance of OSCs was further evaluated. As shown in Fig. 1(d), the OSCs with a structure of ITO/PEDOT:PSS/D18-Cl-BTBHTx (x = 0, 0.05, 0.1, 0.2): Y6/PNDIT-F3N/Ag were fabricated, and the Y6 was chosen as the electron acceptor component because of its complementary absorption spectrum and well-matched energy levels with developed copolymers[42]. As shown in Fig. 3(a), comparable photovoltaic performance could be observed for all D18-Cl-BTBHTx (x = 0, 0.05, 0.1, 0.2): Y6-based devices, and the best PCE of 17.60% was achieved for D18-Cl-BTBHT0.05: Y6-based device. The device based on D18-Cl-BTBHT0.2: Y6 obtained the lowest PCE of 16.61%, which suggests that the excessive copolymerizing ratio of antioxidant BT-BHT unit might adversely affect the efficiency of OSCs. The statistical summary of performance parameters is shown in Table 2. Compared with the device based on D18-Cl: Y6, OSCs based on D18-Cl-BTBHTx (x = 0.05, 0.1, 0.2): Y6 achieved the almost identical short circuit current density (J_{SC}) value of approximately 27.0 mA/cm^2, which demonstrated good consistency with the calculated results from the external quantum efficiency (EQE) spectral integral (Fig. 3(b)). Notably, a significantly lower fill factor (FF) was observed for the device based on D18-Cl-BTBHT0.2: Y6, which was probably due to its inferior active layer morphology (this will be discussed in more detail in the next section). To verify the superiority of incorporating antioxidant BHT group in copolymers than using the BHT as an additive within the active layer, the devices based on D18-Cl: Y6 with the consistent mass fraction of BHT were also fabricated. Their performance is shown in Fig. S18 and the corresponding parameters are summarized in Supplementary Table 1 (Supporting Information). It was demonstrated that the addition of antioxidant BHT tended to degrade the performance of the device. All of the parameters (FF, J_{SC} and V_{OC}), especially FF, were significantly reduced with the increase of antioxidant BHT additives, which can presumably be ascribed to the deterioration of active layer morphology by using the BHT additives. Consequently, with the same weight ratio of antioxidant BHT component, the devices based on the copolymers with BHT-terminated side chains achieved much higher performance than counterparts with BHT as the physical blending additive, which demonstrates the superiority of incorporating antioxidant BHT as linked side chains in ternary copolymers of this work.

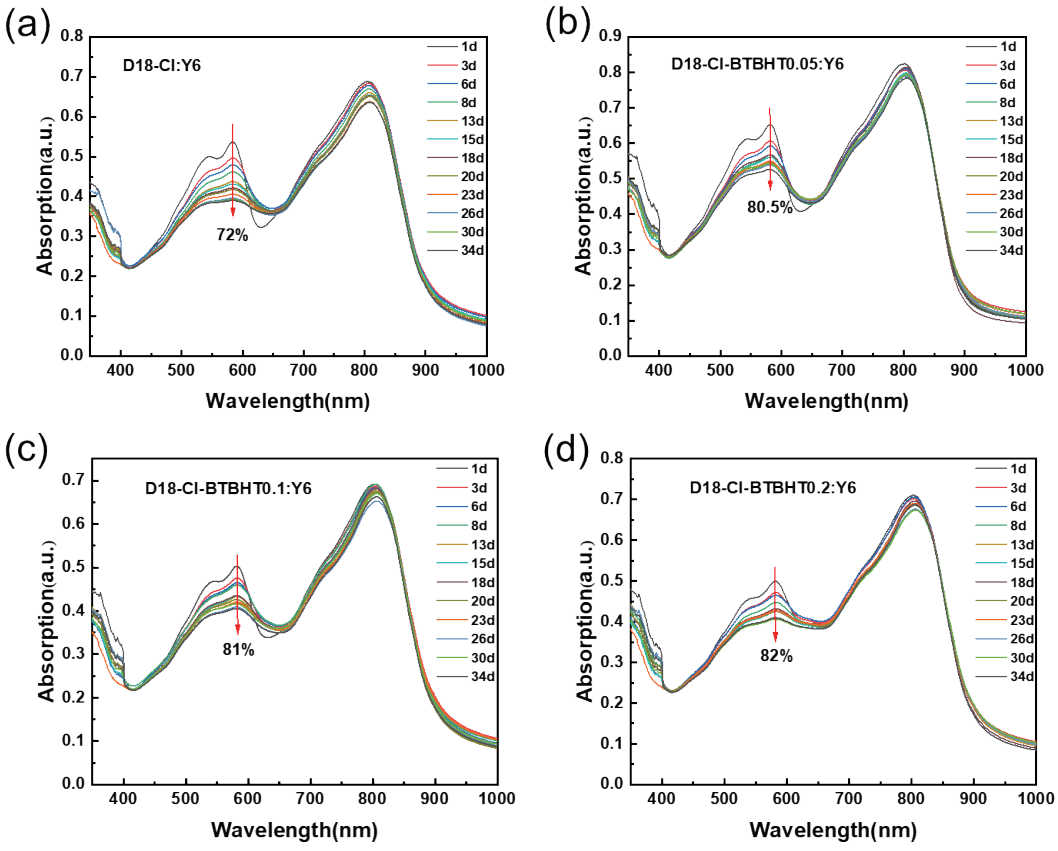

Fig. 2. (Color online) UV absorption spectra of D18-Cl-BTBHTx (x = 0, 0.05, 0.1, 0.2): Y6 blend films under continuous light irradiation at ambient condition, (a) D18-Cl: Y6, (b) D18-Cl-BTBHT0.05: Y6, (c) D18-Cl-BTBHT0.1: Y6, and (d) D18-Cl-BTBHT0.2: Y6 blend film, respectively.

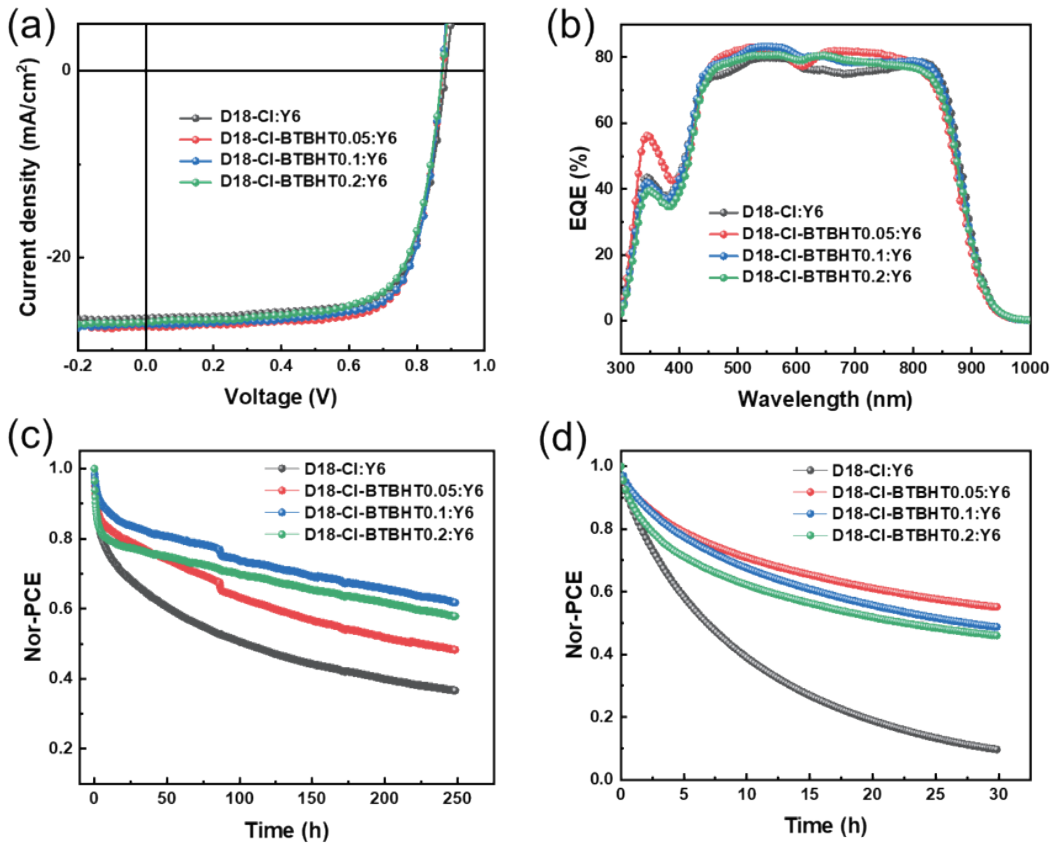

Fig. 3. (Color online) (a) *J-V* characteristics and (b) EQE spectra of the optimized OSCs measured under AM 1.5 G illumination (100 mW/cm^2); PCEs evolution of D18-Cl-BTBHTx: Y6 cells aged at maximum power point (mpp) with continuous light illumination, encapsulated devices (c) in inert atmosphere and unencapsulated devices (d) at ambient conditions.

Table 2. Photovoltaic parameters of D18-Cl-BTBHTx: Y6-based OSCs. [a]

Active layer	V_{OC} (V)	J_{SC} (mA/cm^2)	FF (%)	PCE$_{MAX}$ (%)
D18-Cl: Y6	0.89 (0.88±0.00)	26.92 (26.71±0.18)	72.15 (71.57±0.73)	17.13 (16.91±0.22)
D18-Cl-BTBHT0.05: Y6	0.88 (0.87±0.00)	27.43 (26.98±0.45)	73.25 (72.88±0.33)	17.6 (17.17±0.41)
D18-Cl-BTBHT0.1: Y6	0.88 (0.88±0.00)	27.16 (26.82±0.28)	73.35 (72.66±0.58)	17.41 (17.06±0.25)
D18-Cl-BTBHT0.2: Y6	0.87 (0.87±0.00)	26.95 (26.43±0.42)	70.49 (69.66±0.60)	16.61 (16.07±0.40)

[a] The average data and the corresponding standard deviation were calculated over 12 individual devices.

2.3. Photo-stability of OSCs

The effects of introducing antioxidant BHT side chains on photo-stability of devices were thoroughly investigated. First, OSCs were aged under 250 h continuous illumination with an intensity of 100 mW/cm^2 in a dry inert (N_2) atmosphere at room temperature. The PCE evolution curves of the devices over time is shown in Fig. 3(c). After the 250 h aging treatment, the PCE could maintain 36.6%, 48.2%, 61.7%, and 57.8% of the initial value for the devices based on D18-Cl, D18-Cl-BTBHT0.05, D18-Cl-BTBHT0.1, and D18-Cl-BTBHT0.2, respectively. The control device without the BHT decreased dramatically by almost 64%, whereas the devices with D18-Cl-BTBHTx (x = 0.05, 0.1 0.2) as donor showed improved photo-stability. In particular, the device based on D18-Cl-BTBHT0.1 exhibited the lowest degradation (~38%) in PCE after 250 h aging and displayed an efficiency retention rate that is nearly twice than that of device based on D18-Cl. The detailed variations of specific device parameters under 250 h aging are shown in Fig. S19. The degradation of J_{SC}, FF and V_{OC} could all be suppressed for the devices based on copolymers with antioxidant BHT groups. The long-term stability of unencapsulated OSCs based on these copolymers were also investigated for 30 h storage under ambient conditions. As shown in Fig. 3(d), all of the unencapsulated devices exhibited a faster degradation rate than those in a dry N_2 atmosphere. This indicates that the entry of H_2O and O_2 in the atmosphere is one of the reasons for the photooxidative degradation of OSCs. Nevertheless, the incorporation of BHT-terminated side chains on the copolymers within active layer could significantly enhance the stability of OSCs compared to the control device based on copolymers without BHT-containing chains. The device based on copolymer D18-Cl without BHT-containing chains showed a 90% loss of the initial PCE, whereas only 45%–54% loss of PCEs could be achieved for devices based on copolymers D18-Cl-BTBHTx (x = 0.05, 0.1, 0.2). Therefore, the BHT side chains are proved to play a crucial role in preventing the free radical degradation pathway of the copolymers, which is eventually beneficial for stabilizing the device performance, as reported in previous works[41]. It is worth noting that the reduction of J_{SC} is one of the main derivations for the PCE degradation of devices, which was further verified by long-term monitoring of EQE spectra. As shown in Fig. 4, the decrease in the EQE response strengths was significantly reduced for devices based on copolymers D18-Cl-BTBHTx (x = 0.05, 0.1, 0.2) with BHT side chains after 35 h exposure to light and ambient conditions, especially in the period of the first 15 h. These results strongly demonstrate the efficacy of designing copolymers with BHT side chains for improving the stability of OSCs.

2.4. Charge-carrier dissociation, transport, and recombination dynamics

To elucidate the underlying relationship between attaching BHT-containing side chains on copolymers and photovoltaic performance of OSCs, the dynamics of excitons and charges in the devices were investigated, including exciton dissociation, charge transport, and recombination. As shown in Figs. 5(a) and 5(b), the curves of photocurrent density (J_{ph}) versus effective voltage (V_{eff}) of both as-prepared and aged devices based on copolymers D18-Cl-BTBHTx (x = 0, 0.05, 0.1, 0.2) were measured[47]. For the as-prepared devices, all of the devices exhibited the almost identical J_{ph} versus V_{eff} curves, which suggests similar photocarrier generation for these devices. Accordingly, the charge collection probability P(E, T) under short-circuit conditions was calculated to be over 95% for these as-prepared devices. These results demonstrate that the introduction of BHT-containing side chains would not affect the photocarrier generation and exciton dissociation behaviors of devices before aging, which is consistent with the aforementioned performance results of these devices. Note that after aging of devices for 10 days, slight changes could be observed for the J_{ph} versus V_{eff} curves. The lowest P(E, T) value could be found for the device based on D18-Cl without BHT-containing side chains, which suggests that the introduction of BHT side chains might be useful for maintaining the high photocarrier generation and exciton dissociation for the aged devices.

In addition to the photocarrier generation, the difference in the charge recombination in devices before and after aging was also investigated (Figs. 5(c) and 5(d)). Non-geminate recombination dominates in OSCs, and can be divided into two molecular recombination and trap-assisted recombination[48]. Therefore, the light intensity (P_{light}) dependence of J_{SC} was first determined to evaluate the bimolecular recombination within these devices. According to the power law $J_{SC} \propto P_{light}^{a}$, where a is an exponential factor for representing the degree of bimolecular recombination, and the exponent closer to 1 could indicate the absence of bimolecular recombination within OSCs[49]. As shown in Fig. 5(c), the a values of 0.986, 0.989, 0.991, and 0.989 were calculated for OSCs based on D18-Cl, D18-Cl-BTBHT0.05, D18-Cl-BTBHT0.1, and D18-Cl-BTBHT0.2, respectively. After aging for a period of time, a negligible change could be observed for the a values of all devices (Fig. 5(d)), indicating that the introduction of BHT chains has little effect on the bimolecular recombination loss in devices before and after aging. In addition, the slope of the V_{OC} versus P_{light} curve reflects the property of charge recombination

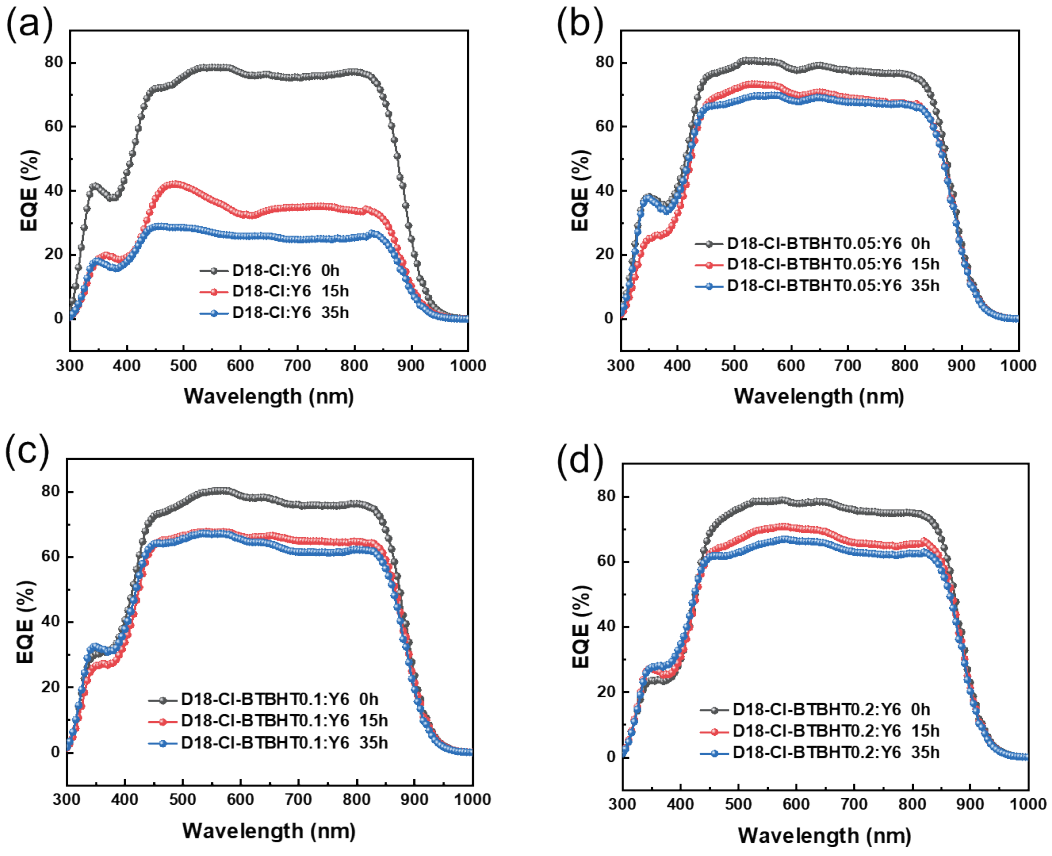

Fig. 4. (Color online) EQEs evolution of D18-Cl-BTBHTx: Y6 cells aged at maximum power point (mpp) under continuous light illumination and ambient conditions; (a) D18-Cl, (b) D18-Cl-BTBHT0.05, (c) D18-Cl-BTBHT0.1 and (d) D18-Cl-BTBHT0.2-based device, respectively.

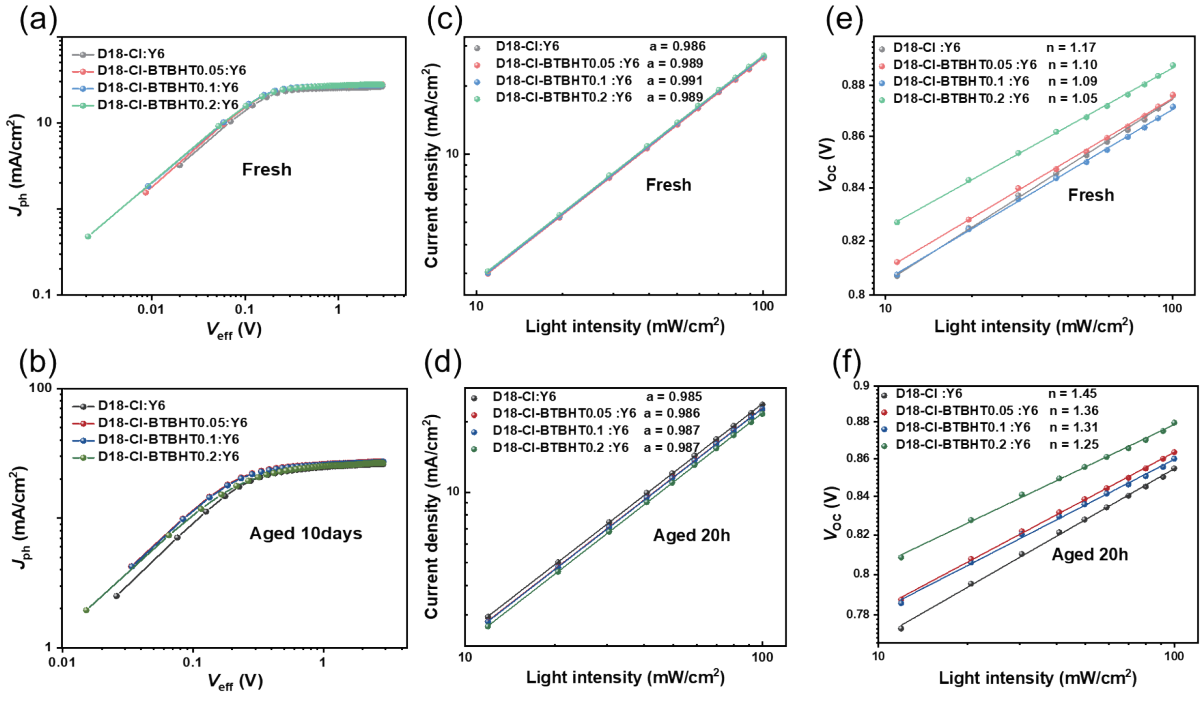

Fig. 5. (Color online) Photocurrent density (J_{ph}) versus effective voltage (V_{eff}) curves of the (a) fresh and (b) aged 10 days D18-Cl-BTBHTx: Y6 cells; light intensity dependence of J_{SC} of the (c) fresh and (d) aged 20 hours D18-Cl-BTBHTx: Y6 cells; light intensity dependence of V_{OC} of the (e) fresh and (f) aged 20 hours D18-Cl-BTBHTx: Y6 cells.

at open-circuit conditions. A curve with a slope of kT/q can be used to evaluate the dominant recombination behavior, where k is the Boltzmann constant, q is the elementary charge and T is the temperature in Kelvin, and the slope of 1 kT/q and 2 kT/q represents the predominant bimolecular recombination and trap-assisted single-molecule recombination, respectively[50]. As shown in Fig. 5(e), slopes of 1.10, 1.09 and 1.05 kT/q were obtained for D18-Cl-BTBHT0.05, D18-Cl-

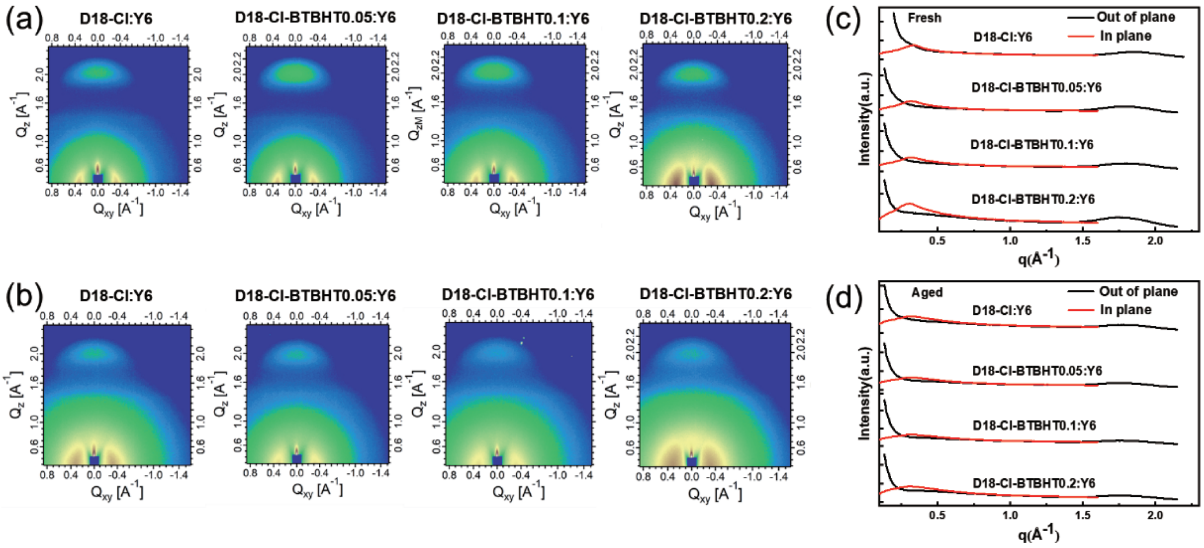

Fig. 6. (Color online) 2D-GIWAXS patterns of (a) as-prepared and (b) aged D18-Cl-BTBHTx: Y6 blend films, 1D line-cut profiles of (c) as-prepared and (d) aged D18-Cl-BTBHTx: Y6 blend films.

BTBHT0.1, and D18-Cl-BTBHT0.2-based devices, respectively, which are slightly lower than the slope of D18-Cl based devices (1.17 kT/q). Note that after a period of aging, the slopes of devices based on D18-Cl-BTBHT0.05, D18-Cl-BTBHT0.1, and D18-Cl-BTBHT0.2 are all significantly lower than that of device based on D18-Cl (Fig. 5(f)). This result demonstrates that the BHT side chains could effectively reduce the trap-assisted recombination for devices after aging, which might be the main reason for the higher FF and J_{SC} for OSCs based on copolymers with BHT side chains during the photooxidation stability tests.

2.5. Morphological properties

To investigate the effect of BHT side chains on the morphology evolution of D18-Cl-BTBHTx: Y6 blend films after aging, two-dimensional (2D) grazing wide-angle X-ray scattering (GIWAXS) measurements were carried out. The corresponding 2D figures and one-dimensional (1D) line-cut profiles of D18-Cl-BTBHTx (x = 0, 0.05, 0.1, 0.2): Y6 blend films before and after aging are shown in Fig. 6. Before aging, similar intermolecular packing behavior could be observed for D18-Cl-BTBHTx (x = 0, 0.05, 0.1, 0.2): Y6 blend films with a peak at 0.32 Å^{-1} in the in-plane (IP) direction and a peak at 1.78 Å^{-1} in the out-of-plane (OOP) direction, resulting in the lamellar stacking distance of ~20 Å and the π-π stacking distance of ~3.5 Å, respectively. This result verifies that the introduction of BHT side chains would not significantly affect the intermolecular packing behaviors within active layers of OSCs before aging, which is consistent with the similar PCEs for these devices. Accordingly, the similar crystal coherence length (CCL) was calculated to be 1.09 nm of the (010) peak and 1.29 nm of the (100) peak. After aging for 140 h at room temperature, the (010) peak intensities of all blend films were slightly weakened while the peak locations were almost unchanged. Therefore, it can be speculated that the morphology alternation might not be the main reason for the PCE decrease for OSCs after aging. Additionally, the space charge-limited current (SCLC) method was used to evaluate the mobility of holes (μ_h) and electrons (μ_e) in D18-Cl-BTBHTx: Y6 blend films, as shown in the Figs. S20a and S20b (Supporting Information)[51]. As shown in Table 3, both μ_h and μ_e were similar and in the same magnitude of 10^{-4} cm^2/(V·s) for all of the blend films. The μ_h/μ_e of 1.84, 1.68, 1.80, and 1.85 was calculated for D18-Cl, D18-Cl-BTBHT0.05, D18-Cl-BTBHT0.1, and D18-Cl-BTBHT0.2 based blends, respectively. It could be found that the D18-Cl-BTBHT0.05: Y6 blend film displayed the most balanced carrier transport, which presumably become one of the reasons for the highest PCE of D18-Cl-BTBHT0.05: Y6-based OSC.

Table 3. The carrier mobilities of blended active-layer films. [a]

	μ_h (10^{-4} cm^2/(V·s))	μ_e (10^{-4} cm^2/(V·s))	μ_h/μ_e
D18-Cl: Y6	6.46	3.50	1.84
D18-Cl-BTBHT0.05: Y6	7.94	4.73	1.68
D18-Cl-BTBHT0.1: Y6	8.27	4.59	1.80
D18-Cl-BTBHT0.2: Y6	6.10	3.30	1.85

[a] Mobility data were measured by the SCLC method.

The surface and overall morphology of the blend films were analyzed by atomic force microscopy (AFM) and transmission electron microscopy (TEM). As shown in Fig. S21, the root mean square (RMS) roughness values of D18-Cl, D18-Cl-BTBHT0.05, D18-Cl-BTBHT0.1, and D18-Cl-BTBHT0.2-based blend films were 1.34, 1.14, 0.99, and 1.04 nm, respectively. Overall, it could be observed that the introduction of BHT-containing side chains on the copolymers would not significantly alter the surface and phase separation morphology of the D18-Cl-BTBHTx: Y6 blend films.

3. Conclusion

In this study, a series of antioxidant ternary copolymers, D18-Cl-BTBHT0.05, D18-Cl-BTBHT0.1 and D18-Cl-BTBHT0.2, were successfully designed and synthesized by incorporating the BT unit with a side chain terminated by an antioxidant BHT group into the conjugated backbone of the widely used donor copolymer D18-Cl. It was found that the introduction of antioxidant BHT group into the side chains of copolymers show superiority for realizing high efficiency of OSCs compared to the strategy of utilizing the BHT as the additive

within active layers. As a result, an optimum PCE of 17.6% could be achieved for the D18-Cl-BTBHT0.05: Y6-based OSC, and a negligible degradation of PCEs could be demonstrated for devices based on D18-Cl-BTBHTx by increasing the BHT ratio from 0.05 to 0.2. It was validated that the attachment of BHT-containing side chains on copolymers could effectively improve the photooxidation stability of OSCs. In particular, the unencapsulated OSC based on D18-Cl-BTBHT0.05: Y6 degraded by only 45% of the initial PCE, significantly outperforming the control device based on D18-Cl: Y6 with 90% PCE degradation after ambient storage for 30 h. The investigation of carrier-generation, charge separation, and transport revealed that BHT side chains could effectively reduce the trap-assisted recombination within OSCs after aging, which eventually results in the excellent retention of J_{SC} and FF for devices after irradiation and storage. This work provides a facile and effective molecular design strategy to developing innovative copolymers for OSCs with simultaneous improvement of efficiency and photooxidation stability.

Acknowledgments

This work was financially supported by National Key Research and Development Program of China (No. 2019YFA0705900) funded by MOST, the Basic and Applied Basic Research Major Program of Guangdong Province (No. 2019B030302007), the National Natural Science Foundation of China (No. U21A6002), and Guangdong-Hong Kong-Macao Joint Laboratory of Optoelectronic and Magnetic Functional Materials (No. 2019B121205002).

Appendix A. Supplementary materials

Supplementary materials to this article can be found online at https://doi.org/1674-4926/44/8/082202.

References

[1] Chen S S, Jung S, Cho H J, et al. Highly flexible and efficient all-polymer solar cells with high-viscosity processing polymer additive toward potential of stretchable devices. Angewandte Chemie Int Ed, 2018, 57(40), 13277

[2] Hou J H, Inganäs O, Friend R H, et al. Organic solar cells based on non-fullerene acceptors. Nat Mater, 2018, 17(2), 119

[3] Kaltenbrunner M, White M S, Głowacki E D, et al. Ultrathin and lightweight organic solar cells with high flexibility. Nat Commun, 2012, 3, 770

[4] Koo D, Jung S, Seo J, et al. Flexible organic solar cells over 15% efficiency with polyimide-integrated graphene electrodes. Joule, 2020, 4(5), 1021

[5] Liu W, Xu X, Yuan J, et al. Low-bandgap non-fullerene acceptors enabling high-performance organic solar cells. ACS Energy Lett, 2021, 6(2), 598

[6] Liu Y H, Liu B W, Ma C Q, et al. Recent progress in organic solar cells (Part II device engineering). Sci China Chem, 2022, 65(8), 1457

[7] Liu Y Q, Qi N, Song T, et al. Highly flexible and lightweight organic solar cells on biocompatible silk fibroin. ACS Appl Mater Interfaces, 2014, 6(23), 20670

[8] Miao J H, Wang Y H, Liu J, et al. Organoboron molecules and polymers for organic solar cell applications. Chem Soc Rev, 2022, 51(1), 153

[9] Murugan P, Hu T, Hu X T, et al. Fused ring A–DA′D–A (Y-series) non-fullerene acceptors: Recent developments and design strategies for organic photovoltaics. J Mater Chem A, 2022, 10(35), 17968

[10] Scharber M C, Mühlbacher D, Koppe M, et al. Design rules for donors in bulk-heterojunction solar cells—Towards 10% energy-conversion efficiency. Adv Mater, 2006, 18(6), 789

[11] Tong Y, Xiao Z, Du X Y, et al. Progress of the key materials for organic solar cells. Sci China Chem, 2020, 63(6), 758

[12] Wadsworth A, Moser M, Marks A, et al. Critical review of the molecular design progress in non-fullerene electron acceptors towards commercially viable organic solar cells. Chem Soc Rev, 2019, 48(6), 1596

[13] Xiao Y F, Zuo C T, Zhong J X, et al. Large-area blade-coated solar cells: Advances and perspectives. Adv Energy Mater, 2021, 11(21), 2100378

[14] Xu B W, Hou J H. Solution-processable conjugated polymers as anode interfacial layer materials for organic solar cells. Adv Energy Mater, 2018, 8(20), 1800022

[15] Xu H T, Yuan F, Zhou D, et al. Hole transport layers for organic solar cells: Recent progress and prospects. J Mater Chem A, 2020, 8(23), 11478

[16] Xue R M, Zhang J W, Li Y W, et al. Organic solar cell materials toward commercialization. Small, 2018, 14(41), 1801793

[17] Zhang G Y, Zhao J B, Chow P C Y, et al. Nonfullerene acceptor molecules for bulk heterojunction organic solar cells. Chem Rev, 2018, 118(7), 3447

[18] Zhang J Q, Tan H S, Guo X G, et al. Material insights and challenges for non-fullerene organic solar cells based on small molecular acceptors. Nat Energy, 2018, 3(9), 720

[19] Zhu L, Zhang M, Zhong W K, et al. Progress and prospects of the morphology of non-fullerene acceptor based high-efficiency organic solar cells. Energy Environ Sci, 2021, 14(8), 4341

[20] Chen S H, Feng L W, Jia T, et al. High-performance polymer solar cells with efficiency over 18% enabled by asymmetric side chain engineering of non-fullerene acceptors. Sci China Chem, 2021, 64(7), 1192

[21] Cui Y, Yao H, Zhang J, et al. Single-Junction organic photovoltaic cells with approaching 18% efficiency. Adv Mater, 2020, 32(19), e1908205

[22] Yuan J, Zhang Y Q, Zhou L Y, et al. Single-junction organic solar cell with over 15% efficiency using fused-ring acceptor with electron-deficient core. Joule, 2019, 3(4), 1140

[23] Wei Y N, Chen Z H, Lu G Y, et al. Binary organic solar cells breaking 19% via manipulating the vertical component distribution. Adv Mater, 2022, 34(33), 2204718

[24] Gao W, Qi F, Peng Z X, et al. Achieving 19% power conversion efficiency in planar-mixed heterojunction organic solar cells using a pseudosymmetric electron acceptor. Adv Mater, 2022, 34(32), 2202089

[25] Zhu L, Zhang M, Xu J Q, et al. Single-junction organic solar cells with over 19% efficiency enabled by a refined double-fibril network morphology. Nat Mater, 2022, 21(6), 656

[26] Burlingame Q, Huang X H, Liu X, et al. Intrinsically stable organic solar cells under high-intensity illumination. Nature, 2019, 573, 394

[27] Du X Y, Heumueller T, Gruber W, et al. Efficient polymer solar cells based on non-fullerene acceptors with potential device lifetime approaching 10 years. Joule, 2019, 3(1), 215

[28] Duan L, Uddin A. Progress in Stability of Organic Solar Cells. Adv Sci, 2020, 7(11), 1903259

[29] Li Y X, Huang X H, Ding K, et al. Non-fullerene acceptor organic photovoltaics with intrinsic operational lifetimes over 30 years. Nat Commun, 2021, 12(1), 5419

[30] Liang Y C, Zhang D F, Wu Z R, et al. Organic solar cells using oligomer acceptors for improved stability and efficiency. Nat Energy, 2022, 7(12), 1180

[31] Xu X, Xiao J, Zhang G, et al. Interface-enhanced organic solar cells with extrapolated T80 lifetimes of over 20 years. Science Bulletin, 2020, 65(3), 208
[32] Rafique S, Abdullah S M, Sulaiman K, et al. Fundamentals of bulk heterojunction organic solar cells: An overview of stability/degradation issues and strategies for improvement. Renew Sustain Energy Rev, 2018, 84, 43
[33] Rivaton A, Tournebize A, Gaume J, et al. Photostability of organic materials used in polymer solar cells. Polym Int, 2014, 63(8), 1335
[34] Jørgensen M, Norrman K, Gevorgyan S A, et al. Stability of polymer solar cells. Adv Mater, 2012, 24(5), 580
[35] Krebs F C. Encapsulation of polymer photovoltaic prototypes. Sol Energy Mater Sol Cells, 2006, 90(20), 3633
[36] Uddin A, Upama M, Yi H M, et al. Encapsulation of organic and perovskite solar cells: A review. Coatings, 2019, 9(2), 65
[37] Oh J, Lee S M, Jung S, et al. Antioxidant additive with a high dielectric constant for high photo-oxidative stabilization of organic solar cells without almost sacrificing initial high efficiencies. Sol RRL, 2021, 5(7), 2000812
[38] Soon Y W, Cho H, Low J, et al. Correlating triplet yield, singlet oxygen generation and photochemical stability in polymer/fullerene blend films. Chem Commun, 2013, 49(13), 1291
[39] Guo J, Wu Y, Sun R, et al. Suppressing photo-oxidation of nonfullerene acceptors and their blends in organic solar cells by exploring material design and employing friendly stabilizers. J Mater Chem A, 2019, 7(43), 25088
[40] Salvador M, Gasparini N, Perea J D, et al. Suppressing photooxidation of conjugated polymers and their blends with fullerenes through nickel chelates. Energy Environ Sci, 2017, 10(9), 2005
[41] Turkovic V, Engmann S, Tsierkezos N, et al. Long-term stabilization of organic solar cells using hindered phenols as additives. ACS Appl Mater Interfaces, 2014, 6(21), 18525
[42] Zeng A P, Ma X L, Pan M G, et al. A chlorinated donor polymer achieving high-performance organic solar cells with a wide range of polymer molecular weight. Adv Funct Mater, 2021, 31(33), 2102413
[43] Qin J, Zhang L, Zuo C, et al. A chlorinated copolymer donor demonstrates a 18.13% power conversion efficiency. J Semicond, 2021, 42(1), 010501
[44] Gong X, Li G W, Wu Y, et al. Enhancing the performance of polymer solar cells by using donor polymers carrying discretely distributed side chains. ACS Appl Mater Interfaces, 2017, 9(28), 24020
[45] Huang X X, Zhang L F, Cheng Y J, et al. Novel narrow bandgap terpolymer donors enables record performance for semitransparent organic solar cells based on all-narrow bandgap semiconductors. Adv Funct Mater, 2022, 32(5), 2108634
[46] Wang Q, Hu Z L, Wu Z H, et al. Introduction of siloxane-terminated side chains into semiconducting polymers to tune phase separation with nonfullerene acceptor for polymer solar cells. ACS Appl Mater Interfaces, 2020, 12(4), 4659
[47] Yu R N, Wei X Q, Wu G Z, et al. Efficient interface modification via multi-site coordination for improved efficiency and stability in organic solar cells. Energy Environ Sci, 2022, 15(2), 822
[48] Vollbrecht J, Brus V V, Ko S J, et al. Quantifying the nongeminate recombination dynamics in nonfullerene bulk heterojunction organic solar cells. Adv Energy Mater, 2019, 9(32), 1901438
[49] Wang Z Q, Hong Z R, Zhuang T J, et al. High fill factor and thermal stability of bilayer organic photovoltaic cells with an inverted structure. Appl Phys Lett, 2015, 106(5), 053305
[50] Koster L J A, Mihailetchi V D, Ramaker R, et al. Light intensity dependence of open-circuit voltage of polymer: Fullerene solar cells. Appl Phys Lett, 2005, 86(12), 123509
[51] Mihailetchi V D, Wildeman J, Blom P W M. Space-charge limited photocurrent. Phys Rev Lett, 2005, 94(12), 126602

Ao Song received her BS degree in engineering from Hunan Normal University in 2020. She is now a Master's student in the State Key Laboratory of Luminescent Materials and Devices in South China University of Technology. Her research focuses on the stability of high-performance organic solar cells.

Qiri Huang received his BS degree from Hefei University of Technology in 2020. He is now a Master's student in the State Key Laboratory of Luminescent Materials and Devices in South China University of Technology. His research focuses on developing high performance inverted organic solar cells.

Chunchen Liu is an associate research fellow in South China University of Technology. He received his BS degree in Polymer Materials and Engineering from South China University of Technology in 2010 and gained his PhD degree in Materials Science from the South China University of Technology in 2005 under the supervision of Prof. Yong Cao. After postdoctoral work at National University of Singapore with Prof. Jishan Wu, he began his academic carrier in 2019 as a research assistant professor of Southern University of Science and Technology and then moved to South China University of Technology in 2021. He mainly focuses on the design and synthesis of conjugated molecules, polymers, and polycyclic aromatic hydrocarbons with polyradicals for opto-electronics.

Fei Huang is a full professor at South China University of Technology. He received his BS degree in Chemistry from Peking University in 2000 and gained his PhD degree in Materials Science from the South China University of Technology in 2005 under the supervision of Prof. Yong Cao. After postdoctoral work at University of Washington with Prof. Alex K.-Y. Jen, he began his academic career in 2009 as a professor of South China University of Technology. His main interests are in organic functional materials and devices for opto-electronics.